

PhenoKG: Knowledge Graph-Driven Gene Discovery and Patient Insights from Phenotypes Alone

Kamilia Zaripova ^{*1,2} Ege Özsoy ^{1,2} Nassir Navab ^{1,2,3} Azade Farshad ^{1,2}

¹Department of Computer Science, Technical University of Munich

²Munich Center for Machine Learning (MCML), Munich, Germany

³Johns Hopkins University, Baltimore, Maryland, USA

June 17, 2025

Abstract

Identifying causative genes from patient phenotypes remains a significant challenge in precision medicine, with important implications for the diagnosis and treatment of genetic disorders. We propose a novel graph-based approach for predicting causative genes from patient phenotypes, with or without an available list of candidate genes, by integrating a rare disease knowledge graph (KG). Our model, combining graph neural networks and transformers, achieves substantial improvements over the current state-of-the-art. On the real-world MyGene2 dataset, it attains a mean reciprocal rank (MRR) of 24.64% and nDCG@100 of 33.64%, surpassing the best baseline (SHEPHERD) at 19.02% MRR and 30.54% nDCG@100. We perform extensive ablation studies to validate the contribution of each model component. Notably, the approach generalizes to cases where only phenotypic data are available, addressing key challenges in clinical decision support when genomic information is incomplete.

1 Introduction

With over 300 million individuals affected globally, rare genetic disorders represent a profound challenge for healthcare systems, largely due to their low incidence and wide-ranging symptoms [Nguengang Wakap et al., 2020]. Even with rapid developments in genomic science, the path to an accurate diagnosis is often long and convoluted, frequently requiring years of medical appointments and consultations with various specialists [Adams et al., 2024]. This extended diagnostic process—often referred to as a "diagnostic odyssey"—is made more difficult by the limited number of experts in the field, the absence of unified diagnostic criteria, and the scarcity of annotated datasets necessary for training AI-driven diagnostic tools [Decherchi et al., 2021]. As a consequence, approximately 70% of patients in search of a diagnosis remain without one, and the genetic causes of nearly half of all Mendelian conditions—those resulting from mutations in a single gene—remain unidentified [Gahl et al., 2012, Chong et al., 2015]. These delays not only increase the likelihood of unnecessary or repetitive testing but also hinder timely intervention, often leading to preventable deterioration in patient health.

Seminal and recent studies on rare genetic diseases have shown that pinpointing the pathogenic variant in a gene responsible for a patient's condition greatly improves diagnostic accuracy and informs downstream clinical management [Boycott et al., 2013, Posey et al., 2019]. Historically, clinicians manually integrated structured and unstructured clinical observations—spanning physical traits, symptom trajectories, and laboratory findings—with genomic data produced by exome or genome sequencing [James et al., 2016]. Although many centres now employ semi-automated decision-support pipelines using methods for identification of potential patients with rare conditions, like [Prakash et al., 2021, Thompson et al., 2023], expert interpretation remains indispensable. The collection of observable characteristics (the phenotype) provides essential context for interpreting the genotype—the individual's complete set of genetic variants—which often contains variants of uncertain significance. When a pathogenic or likely pathogenic variant is

*Corresponding author: kamilia.zaripova@tum.de

identified in a gene whose gene-disease relationship is rated Definitive or Strong and whose known disease spectrum fits the patient’s phenotype, that variant can be considered causative under ACMG/AMP and ClinGen criteria [Richards et al., 2015, Strande et al., 2017]. This information is crucial not only for diagnosis but also for prognosis, genetic counseling, and, in selected cases, therapeutic decision-making.

Despite advances in sequencing, variant-effect prediction, and phenotype-driven gene prioritisation, overall diagnostic yields for rare Mendelian disorders still hover around 30–50%—and are lower in under-represented ancestries and in atypical clinical presentations. These persistent gaps underscore the need for next-generation machine-learning models, graph-based approaches, and multimodal frameworks that can integrate heterogeneous biomedical data at scale while preserving clinical interpretability and portability across diverse populations [Decherchi et al., 2021].

Most diagnostic pipelines assume that clinicians have already narrowed the search to a hand-curated list of “candidate” genes harboring patient-specific DNA variants—an approach limited by current medical knowledge and expertise, and requiring substantial manual effort. We present a scalable alternative that starts from a patient’s phenotype terms, enriches them with a biomedical knowledge graph (KG), and ranks ≈ 8000 genes by their probability of being causative. This serves as either a direct prediction method or as a pre-filter to help clinicians avoid testing variants across the entire genome. We focus on Mendelian diseases with a single causative gene. Without a pre-filtered list, the model achieves $15.15 \pm 3.33\%$ accuracy (correct gene among the top-ranked suggestions). With an optional expert-curated variant (candidate) list (≈ 20 genes), accuracy rises to $83.96 \pm 1.45\%$. The constructed patient graph structure enables the model to suggest genes for the prioritization evaluation outside expert-curated lists, capturing patient-specific phenotype-disease-genotype relationships. In theory, this provides clinicians with an additional discovery layer; however, this requires prospective validation, as only follow-up variant testing can confirm the predictions.

Our contributions are summarized as follows:

1. We introduce PhenoKG, a method that captures patient-specific uniqueness via graph structures and gene representations, outperforming current state-of-the-art approaches.
2. We demonstrate that our model performs well both with and without a candidate list through quantitative evaluation.
3. Our experiments show that models trained solely for causative gene prediction underperform on patient-like retrieval tasks when evaluated by true gene alone. However, strong performance on the primary task suggests that patients grouped closely in embedding space may share common biological characteristics beyond a single gene, which warrants further investigation.

2 Related Works

To address diagnostic odysseys, researchers have explored three main machine learning strategies: genotype-based methods, phenotype-based methods, and hybrid models. Genotype-based Methods leverage genomic sequencing data to identify variants associated with specific diseases. Techniques such as variant frequency analysis, pathogenicity prediction, and gene-disease databases are commonly used. Tools like MutationTaster [Steinhaus et al., 2021], CADD [Rentzsch et al., 2019], and M-CAP, a clinical pathogenicity classifier [Jagadeesh et al., 2016], have shown utility but are limited by the need for comprehensive variant annotations and training data.

Phenotype-driven tools prioritize diseases or genes by comparing a patient’s phenotypic abnormalities to curated knowledge bases like Phenolyzer [Yang et al., 2015, Köhler et al., 2009] that use prior information to implicate genes involved in diseases and others [Jagadeesh et al., 2019, Peng et al., 2021, Rao et al., 2018]. Facial phenotyping tools like DeepGestalt [Gurovich et al., 2019], GestaltMatcher [Hsieh et al., 2022], PEDIA [Hsieh et al., 2019], and others [Duong et al., 2022, Hong et al., 2021, Shukla et al., 2017] have demonstrated the potential to bridge phenotype-genotype associations, though they often struggle with complex or novel presentations.

Hybrid approaches combining genotype and phenotype data have improved diagnostic accuracy, including Bayesian frameworks integrating probabilities from multiple data sources [Robinson et al., 2020, Javed et al., 2014] and deep learning models predicting disease or gene likelihood from phenotype-genotype associations [Smedley et al., 2015, Li et al., 2019, Birgmeier et al., 2020, Yoo et al., 2021, Anderson et al., 2019]. A recent example is AI-MARRVEL (AIM) [Mao et al., 2024], a random forest that ranks variants genome-wide by combining patient variant-call files with Human Phenotype Ontology (HPO) terms. In contrast, PhenoKG operates without sequencing data, prioritizing genes rather than variants. Using only phenotype data and a knowledge graph, it serves as an upstream triage tool to reduce clinicians’ search space, accelerate gene prioritization, and surface plausible candidate genes beyond curated panels.

Other methods, such as Shepherd [Alsentzer et al., 2022] and CADA [Peng et al., 2021], leverage KGs to enrich patient information. CADA builds a phenotype–gene KG, learns Node2Vec embeddings, and ranks candidate genes

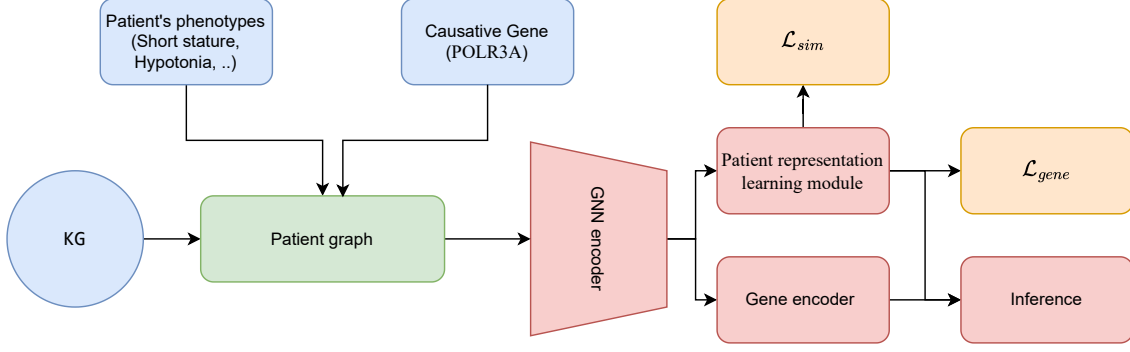


Figure 1: Overview of PhenoKG for rare disease gene prioritization. The model constructs a patient-specific subgraph using phenotypes and a knowledge graph. GATv2 layers generate node embeddings, which are used to create patient and gene representations. These feed into loss functions to predict the most likely causative gene.

by embedding similarity to patient HPO term vectors. Like our approach, CADA requires only phenotype data but underperforms compared to Shepherd due to KG design and model choices; thus, we benchmark only against Shepherd. Shepherd introduces three models with shared pre-training for disease prediction, gene prioritization, and “patient-like-me” prediction; we focus solely on gene prioritization. Shepherd pre-trains a KG encoder via link prediction, then adds a downstream gene-ranking model. A key limitation is its reliance on an external candidate gene list, either expert-curated or generated by additional tools.

3 Method

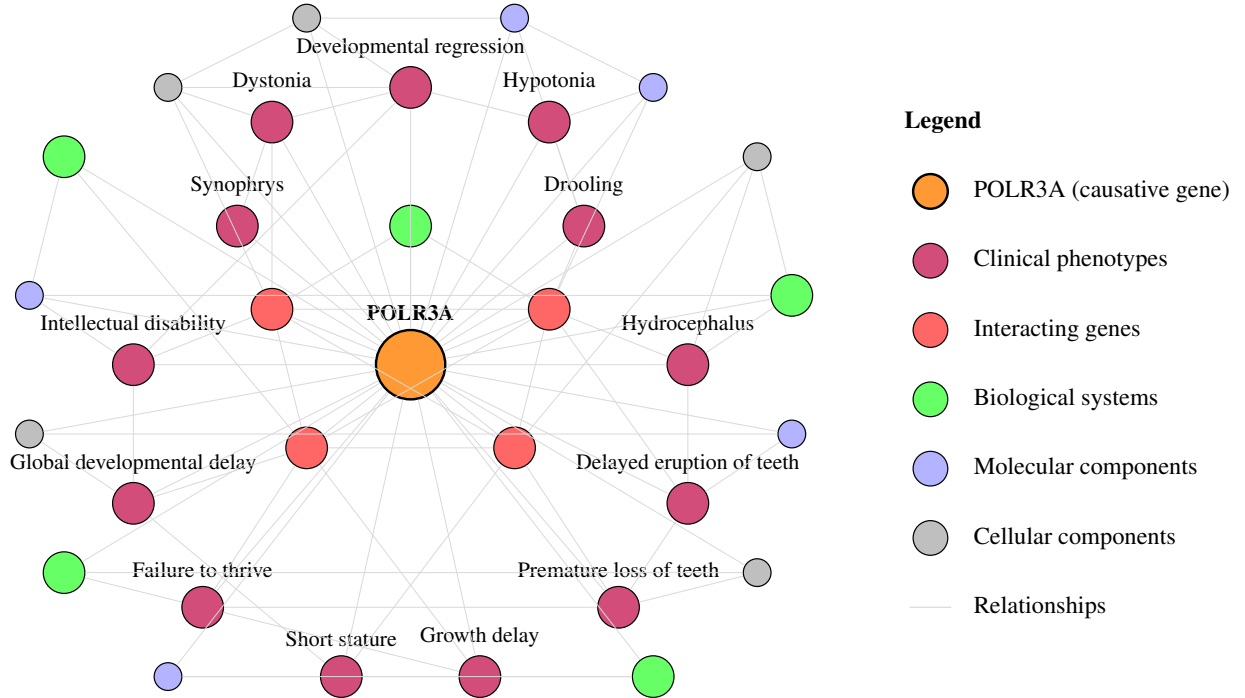


Figure 2: An example of a simplified patient-specific one-hop subgraph and its neighborhood, illustrating the relationships between the *POLR3A* gene and associated genes, diseases, and phenotypes. The real patient subgraph maintains a similar structure but is substantially more complex.

We propose PhenoKG, a framework for predicting the causative gene in rare monogenic diseases by prioritizing genes associated with patient phenotypes. Our approach leverages the PrimeKG knowledge graph G [Chandak et al., 2023] to

model gene-phenotype relationships. Specifically, PhenoKG learns informative representations from patient-specific subgraphs G_p , which uniquely represent a patient based on their list of phenotypes and a set of candidate genes provided by clinicians or obtained from the knowledge graph. The patient subgraph is further augmented with additional information from the knowledge graph, such as related diseases and other relevant entities. As output, the model provides a ranked list of candidate genes, each associated with a relevance score indicating its likelihood of being causative for the patient. An overview of the proposed method is shown in Figure 1.

3.1 Problem Formulation

Given a patient p with an associated set of phenotypes \mathcal{P}_p , encoded using the Human Phenotype Ontology (HPO) system (e.g., [HP:0004322, HP:0001263, ...]), and a complete candidate gene set \mathcal{G} (e.g., [ENSG00000123066, ENSG00000141510, ...]), the set \mathcal{G} with the goal of identifying the causative gene $g^* \in \mathcal{G}$ responsible for the patient’s condition (e.g., $g^* = \text{ENSG00000165588}$, which corresponds to the *OTX2* gene).

For each patient, the candidate gene list can be extracted from the global knowledge graph G , either based on phenotype-gene associations or as specified by clinicians. The global knowledge graph G is represented as an undirected graph defined by $G = (X, E, A)$, where $X \in \mathbb{R}^{N \times d_{\text{in}}}$ denotes the set of node features, with N being the number of nodes in KG and d_{in} the feature dimension. Each node, corresponding to a gene, phenotype, or other biomedical entity, is initialized with a unique embedding obtained by pretraining G on a link prediction task, as described in [Alsentzer et al., 2022]. The set E represents the edges capturing relationships between nodes, such as phenotype-gene associations and gene-gene interactions. The matrix A defines the connectivity structure of the graph and is described in detail in Section 4.1.

3.2 Patient-specific Subgraphs

To construct the patient-specific subgraph G_p , we compute the shortest paths from each phenotype $p_i \in \mathcal{P}_p$ to a provided or inferred list of candidate genes. The subgraph G_p includes all nodes along these paths, along with any additional nodes required to ensure connectivity. If no candidate gene list is available, the k -hop neighborhood can be extracted for each phenotype from G , and all genes within this neighborhood are treated as candidates. Formally, G_p is represented as (X_p, E_p, A_p) , where $X_p \subseteq X$, $E_p \subseteq E$, and $A_p \subseteq A$. Here, $X_p \in \mathbb{R}^{n \times d_{\text{in}}}$ denotes the node feature matrix, $E_p \subseteq \{1, \dots, n\}^2$ represents the edge set with the n nodes in G_p , and $A_p \in \mathbb{R}^{|E_p| \times d_e}$ contains the edge attributes corresponding to E_p , an example of the patient subgraph is illustrated Figure 2.

3.2.1 Model

GNN module For each G_p , we apply a multi-layer graph convolutional network encoder to refine the original node embeddings. Let $H^{(0)} = X_p$ denote the initial node features. Node representations are updated across L layers as follows:

$$H^{(l)} = \text{Dropout} \left(\sigma \left(\text{LayerNorm} \left(\text{GATv2}(H^{(l-1)}, E, A) \right) \right) \right), \quad l = 1, \dots, L-1,$$

where $\sigma(\cdot)$ is a non-linear activation function, $\text{LayerNorm}(\cdot)$ denotes layer normalization, and $\text{Dropout}(\cdot)$ is a dropout operation applied for regularization during training. The final node representations are projected via a learnable linear map (f_{proj}):

$$Z = f_{\text{proj}} \left(\text{GATv2}(H^{(L-1)}, E, A) \right).$$

The GATv2 is an attention graph operator from [Brody et al., 2022].

Let $\{z_i\}_{i=1}^n$ be the node embeddings output by the GNN module. We partition these into phenotype and gene sets.

Patient representation learning module Phenotype embeddings are first projected by a multi-layer perceptron (MLP), denoted by f_{pheno} :

$$\tilde{z}_i = f_{\text{pheno}}(\{z_i\}_{i \in \mathcal{P}_p}).$$

To incorporate global context, m learnable memory vectors $M \in \mathbb{R}^{m \times d}$ are concatenated with the phenotype embeddings and passed through multi-head self-attention:

$$\hat{Z} = \text{MHA}([\tilde{Z}; M]),$$

where MHA denotes standard multi-head attention as introduced in [Vaswani et al., 2017].

The patient representation $p \in \mathbb{R}^d$ is then obtained by masked mean pooling over phenotype nodes, followed by a two-layer MLP denoted by f_{patient} :

$$p = f_{\text{patient}} \left(\frac{1}{|\mathcal{P}_p|} \sum_{i \in \mathcal{P}_p} \hat{Z}_i \right).$$

Gene Encoder Gene node embeddings are processed via a Transformer-based encoder [Vaswani et al., 2017], parameterized by θ :

$$\mathbf{G} = \theta(\{z_j\}_{j \in \mathcal{G}_p}),$$

where \mathcal{G}_p are the gene indices in the patient graph and $\mathbf{G} \in \mathbb{R}^{L \times d}$ are gene embeddings.

3.3 Losses

Gene Loss To train the model, we adopt a contrastive loss framework. Let $p \in \mathbb{R}^d$ be the patient embedding, $\mathbf{G} = [g_1, \dots, g_L] \in \mathbb{R}^{L \times d}$ the candidate gene embeddings, and g^* the embedding of the causative gene. All embeddings are normalized to unit norm. We compute cosine similarities, where τ is a learnable temperature parameter:

$$\text{sim}(p, g_i) = \frac{\langle p, g_i \rangle}{\tau},$$

Let $\text{sim}^* = \text{sim}(p, g^*)$ be the similarity to the true gene. We apply semi-hard negative mining by first selecting a candidate set of negative genes satisfying:

$$\text{sim}(p, g^-) < \text{sim}^* - \gamma,$$

where γ is a margin hyperparameter. Among this candidate set, we select the negative gene with the highest similarity (i.e., the hardest semi-hard negative). If no semi-hard candidate exists, we select the negative gene with the highest overall similarity. This strategy balances learning from informative negatives while avoiding extreme outliers.

The loss is then computed using a margin-based triplet loss:

$$\mathcal{L}_{\text{triplet}} = \max(0, \text{sim}(p, g^-) - \text{sim}(p, g^*) + \gamma).$$

We further add an L2 norm regularization term to encourage both patient and gene embeddings to remain close to unit norm:

$$\mathcal{L}_{\text{reg}} = \lambda \left(\|p\|_2 + \text{mean}(\|\mathbf{G}\|_2) - 2 \right),$$

where λ is a regularization weight and $\|\mathbf{G}\|_2$ is the mean L2 norm across candidate gene embeddings.

The total loss is:

$$\mathcal{L}_{\text{gene}} = \mathcal{L}_{\text{triplet}} + \mathcal{L}_{\text{reg}}.$$

Patient Similarity Loss To encourage consistency across batches and improve generalization, we maintain a memory bank \mathcal{M} of past patient embeddings and their associated gene labels. Let $\mathcal{M} = \{(p_i, g_i)\}$ be the set of embeddings in the memory bank.

The patient similarity loss is computed based on cosine similarities between patient embeddings having the same causative gene in the current and previous batches. We define:

$$\mathcal{L}_{\text{sim}} = \mathcal{L}_{\text{within}} + \mathcal{L}_{\text{cross}},$$

where $\mathcal{L}_{\text{within}}$ compares embeddings within the current batch, and $\mathcal{L}_{\text{cross}}$ compares them against the memory bank.

Each of $\mathcal{L}_{\text{within}}$ and $\mathcal{L}_{\text{cross}}$ consists of two parts: pulling same-gene pairs together and pushing different-gene pairs apart.

$$\begin{aligned} \mathcal{L}_{\text{pull}} &= -\log \sigma \left(\frac{\text{sim}(p_i, p_j)}{\alpha} \right), \quad \text{for } g_i = g_j \\ \mathcal{L}_{\text{push}} &= \max(0, \delta - (1 - \text{sim}(p_i, p_j))) \quad \text{for } g_i \neq g_j \end{aligned}$$

The final loss becomes:

$$\mathcal{L}_{\text{total}} = \mathcal{L}_{\text{gene}} + \mathcal{L}_{\text{sim}},$$

with δ the margin and α the temperature. The memory bank is updated per batch using a circular buffer strategy to retain a fixed number of embeddings.

3.4 Inference

At inference time, we construct the patient-specific subgraph G_p by extracting the k -hop neighborhood around each phenotype in \mathcal{P}_p , thereby capturing the set of candidate genes \mathcal{G}_p associated with the patient’s clinical profile (Section 3.2). The model encodes G_p to produce a patient embedding p and gene embeddings $\mathbf{G} = \{g_j\}_{j \in \mathcal{G}_p}$.

Relevance scores are computed via:

$$\text{sim}(p, g_j) = \langle p, g_j \rangle, \quad \forall j \in \mathcal{G}_p.$$

The final output is a ranked list of candidate genes:

$$\mathcal{G}_p^{\text{ranked}} = \text{argsort}_{j \in \mathcal{G}_p} (\text{sim}(p, g_j)).$$

4 Experiments and Results

4.1 Dataset

We used two datasets in our experiments. The model was trained on a simulated dataset from [Alsentzer et al., 2023], which includes training (36,224 patients) and validation (6,080 patients) splits. Simulated data was chosen for its similarity to the Undiagnosed Diseases Network (UDN) dataset [Ramoni et al., 2017], its larger size for training complex models, and its public availability, unlike most real datasets except MyGene2 ([University of Washington, Center for Mendelian Genomics]). A random subset of 320 patients from the original validation set was used as a final test set. Each simulated patient includes positive phenotypes and a challenging candidate gene list. Patients with causative genes missing from the knowledge graph were excluded from training. While our method theoretically can assess previously unseen genes, this requires the new gene to be manually connected to the existing KG (e.g., via related genes or diseases), which allows information and embeddings to propagate without the need to retrain the entire model, however, investigating the performance of it lies beyond the scope of the current work.

The second test dataset is the real-world MyGene2 set, originally comprising 146 patients and 48 unique causal genes, with an average of 7.9 ± 6.6 phenotypes per patient. Data collection and preprocessing followed [Alsentzer et al., 2022]. As MyGene2 lacks expert-curated candidate gene lists, we used it to test model performance without candidate genes. For efficiency, we restricted evaluation to the two-hop neighborhood around each patient; patients whose causative gene was unreachable within two hops were excluded, leaving 121 patients. It is worth noting that the simulated dataset is similar in structure to the patients in the UDN [Alsentzer et al., 2023], as it was generated based on and compared to it. However, it differs significantly from the MyGene2 dataset. Unlike MyGene2, the simulated dataset provides a list of candidate genes for each patient. Consequently, the patient subgraphs in the two datasets differ in both structure and size.

Our method uses a knowledge graph (KG) to augment patient information and identify candidate genes. We employed PrimeKG, developed in [Chandak et al., 2023] and adapted for rare disease tasks in [Alsentzer et al., 2022], comprising 105,220 nodes and 1,095,469 edges. Nodes represent seven biological entity types: phenotypes (15,874), diseases (21,233), genes/proteins (21,610), pathways (2,516), molecular functions (11,169), cellular components (4,176), and biological processes (28,642), defined by biomedical vocabularies such as HPO [Köhler et al., 2019] and ENSEMBL [Aken et al., 2016], among others. Edges span 17 relation types, including protein-protein interactions (321,075), disease-phenotype (204,779 positive, 1,483 negative), phenotype-phenotype (21,925), phenotype-protein (10,518), and disease-protein associations (86,299), among others. Full KG details are in [Chandak et al., 2023, Alsentzer et al., 2022].

We use the terms *gene* and *protein* in this section interchangeably, as genes are represented by their encoded proteins in the knowledge graph. This reflects that most biological interaction data, such as protein-protein interactions and functional annotations, are defined at the protein level. Thus, gene references correspond to protein nodes acting as proxies for genes.

4.2 Implementation Details

We pre-trained the global graph G on a link prediction task [Alsentzer et al., 2022] with 512-dimensional output embeddings. The GNN module used $L = 3$ GATv2 [Brody et al., 2022] layers with $h = 2$ attention heads per layer, hidden dimensions $d_{\text{hid}}^{(1)} = 1024$, $d_{\text{hid}}^{(2)} = 256$, and output $d_{\text{out}} = 512$. LayerNorm [Ba et al., 2016] and LeakyReLU [Maas et al., 2013] were applied between layers, with dropout $p = 0.4$. Edge attributes ($d_e = 15$) were incorporated into the attention mechanism to enhance relational modeling, and a final linear transformation was applied to project the resulting node representations into the output embedding space.

For patient representation learning, phenotype projection f_{pheno} used a two-layer MLP with ReLU [Krizhevsky et al., 2012] and LeakyReLU. The memory bank contained $m = 128$ learnable vectors (normal init., mean 0, std 1). Phenotype attention used 4 attention heads. Patient embeddings were aggregated and passed through a two-layer MLP with LeakyReLU. Gene embeddings were processed by a transformer encoder [Vaswani et al., 2017] with 4 layers, 8 attention heads, and an intermediate size of 2048. Model training was performed using the AdamW optimizer [Loshchilov and Hutter, 2017] with a learning rate of 1×10^{-4} , combined with a cosine annealing learning rate scheduler [Loshchilov and Hutter, 2016] configured with $T_0 = 10$ and a multiplier $T_{\text{mult}} = 2$. The patient neighbourhood was defined using $k = 2$ nearest neighbours. The following hyperparameters were used: margin $\gamma = 0.3$, contrastive temperature $\tau = 0.12$, regularization weight $\lambda = 0.03$, patient similarity temperature $\alpha = 0.5$, and similarity margin $\delta = 0.8$. All models were implemented and trained using PyTorch, PyTorch Geometric, and Transformers. Encoder training ran for up to 135 epochs with early stopping after 25 epochs.

4.3 Evaluation Metrics

We evaluated our model using Mean Reciprocal Rank (MRR) and normalized Discounted Cumulative Gain (nDCG) [Järvelin and Kekäläinen, 2002]. MRR calculates the inverse rank of the first correct gene for each case and averages across cases, offering smooth sensitivity to ranking changes. nDCG accounts for the relevance of all ranked genes, applying a logarithmic penalty to lower ranks and normalizing against an ideal ranking, with scores ranging from 0 to 1. It places greater importance on highly ranked relevant genes, making it particularly informative for prioritization tasks. In contrast, $\text{hits}@j$ simply checks whether the correct gene appears within the top j positions, ignoring rankings beyond that threshold.

4.4 Results and Discussions

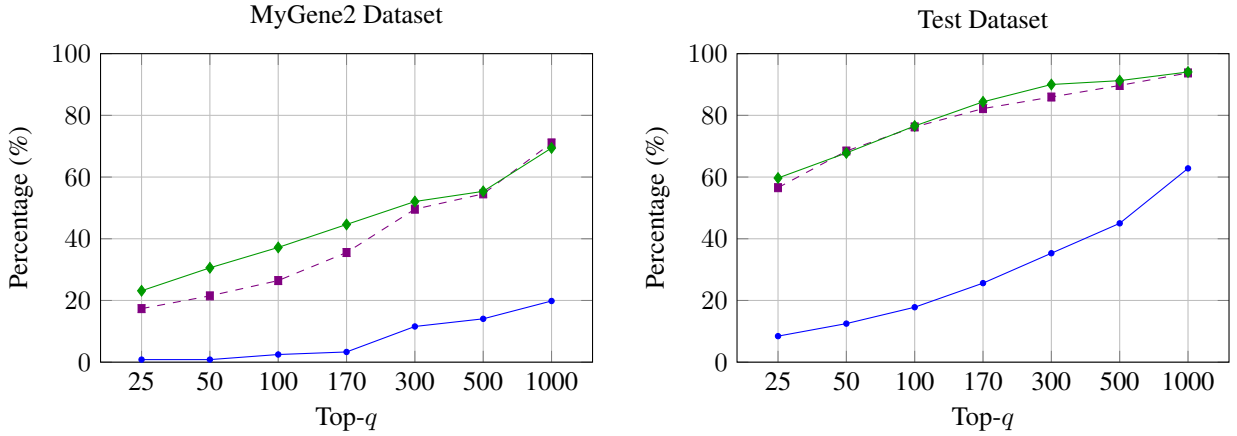


Figure 3: Match percentage comparison for MyGene2 (left) and simulated test (right) datasets, across top- q values. Blue solid line with circles: PhenoKG with $\mathcal{L}_{\text{gene}}$; violet dashed line with squares: with combined \mathcal{L} loss; green line with diamonds: model with \mathcal{L}_{sim} .

The proposed model and the competitive Shepherd model [Alsentzer et al., 2022] were evaluated under the same experimental setup, data splits, and preprocessing protocols. Shepherd was selected for comparison due to its use of knowledge graphs and its superior performance over other models [Alsentzer et al., 2022]. We tested multiple configurations of our model using different combinations of loss functions: gene loss only, patient similarity loss only, and a combined loss. Additionally, we assessed variants using three embedding strategies: (1) *Pretrained Embeddings*, where node embeddings were initialized from link prediction pretraining; (2) *No Embeddings*, with randomly initialized embeddings; and (3) *Only Patient Phenotypes*, where only real patient phenotype nodes were used for subgraph construction and the model used pretrained embeddings. The *Pretrained Embeddings* and *No Embeddings* configurations included all phenotypes in the patient graph. Each configuration was trained three times, and we report the mean performance along with the standard deviation.

We also evaluated causative gene identification via patient similarity: each test patient embedding was compared to training and validation embeddings, with top- q matches assessed for shared causative genes (Figure 3). It is important to note that the MyGene2 and simulated test datasets differ in graph structure. MyGene2 includes portions of the KG not seen during training. Pretraining was shown to be not critical when training data covered the full KG or for deployment

Table 1: Evaluation results using MRR and nDCG@K (in %) are reported across different model groups for the simulated test dataset compared to SHEPHERD [Alsentzer et al., 2022]. Higher values indicate better performance. The *Pretrained embeddings* group corresponds to training initialized with embeddings pretrained on the knowledge graph for a link prediction task. The *No embeddings* group refers to training from scratch. The *Only patient phenotypes* group includes models trained solely on original patient phenotype data. Rows within each group represent different training setups using various loss function combinations.

Model	MRR (%) \uparrow	nDCG@1 \uparrow	nDCG@3 \uparrow	nDCG@5 \uparrow	nDCG@10 \uparrow	nDCG@25 \uparrow
Competitive Method						
SHEPHERD	79.35 \pm 0.00	66.88 \pm 0.00	80.07 \pm 0.00	82.77 \pm 0.00	84.26 \pm 0.00	84.43 \pm 0.00
PhenoKG (Ours)						
$\mathcal{L}_{\text{gene}} \mathcal{L}_{\text{sim}}$						
<i>No Embeddings</i>						
✓ ✗	85.32 \pm 1.52	76.67 \pm 2.70	86.55 \pm 1.15	87.73 \pm 1.13	88.91 \pm 1.18	88.94 \pm 1.14
✗ ✓	86.81 \pm 0.84	79.69 \pm 0.68	87.54 \pm 1.10	88.91 \pm 0.90	89.69 \pm 0.78	90.01 \pm 0.66
✓ ✓	86.60 \pm 1.36	79.27 \pm 1.50	87.45 \pm 1.61	88.73 \pm 1.31	89.41 \pm 1.16	89.84 \pm 1.06
<i>Only Patient Phenotypes</i>						
✓ ✗	89.54 \pm 0.45	83.85 \pm 0.78	90.00 \pm 0.26	91.08 \pm 0.28	91.86 \pm 0.27	92.07 \pm 0.33
✗ ✓	91.08 \pm 0.71	86.98 \pm 0.74	91.26 \pm 1.01	92.22 \pm 0.68	92.88 \pm 0.49	93.20 \pm 0.56
✓ ✓	90.37 \pm 0.92	85.10 \pm 0.90	90.95 \pm 1.15	91.73 \pm 0.73	92.38 \pm 0.82	92.70 \pm 0.72
<i>Pretrained Embeddings</i>						
✓ ✗	89.81 \pm 0.77	84.27 \pm 1.54	90.23 \pm 0.60	91.23 \pm 0.47	92.10 \pm 0.53	92.28 \pm 0.57
✗ ✓	91.61 \pm 1.05	87.19 \pm 1.42	92.03 \pm 1.10	92.76 \pm 0.88	93.32 \pm 0.81	93.63 \pm 0.80
✓ ✓	89.15 \pm 0.92	83.96 \pm 1.45	89.20 \pm 0.91	90.58 \pm 0.81	91.36 \pm 0.57	91.74 \pm 0.69

on similar datasets (Table 1), but was necessary for generalization to novel phenotype-gene combinations in MyGene2 (Table 2). On the simulated dataset, the *Only Patient Phenotypes* model trained with similarity loss achieved an MRR of $91.08 \pm 0.71\%$ and nDCG@1 of $86.98 \pm 0.74\%$, outperforming Shepherd (MRR 79.35%, nDCG@1 66.88%). On MyGene2, the *Pretrained Embeddings* model with combined loss obtained the best performance (MRR $24.64 \pm 4.57\%$, nDCG@1 $15.15 \pm 3.33\%$), compared to Shepherd (MRR 19.02%, nDCG@1 11.57%).

We compared three loss function configurations. Models trained solely with gene loss performed well on the causative gene prediction task but poorly on the auxiliary patient similarity task (Figure 3). Models trained solely with patient similarity loss excelled at patient similarity-based gene identification and delivered competitive results on causative gene prediction, with only a minor drop in top-nDCG performance. The observed behavior can be attributed to the absence of alignment between patient embeddings across batches, which led to divergent representations even among patients sharing the same causative gene. Each patient’s unique graph structure causes patient embeddings to capture both shared and distinct attributes.

Models trained with the combined loss delivered the most robust and consistent performance on the MyGene2 dataset by enforcing alignment across patient representations while preserving individuality. This observation suggests an interesting direction for future work: understanding how patient embeddings relate when causative genes differ. If a model trained solely with gene loss yields patient representations that still cluster meaningfully, what other aspects of patient phenotype space are being captured? As our quantitative results suggest, patient embeddings encode more than just gene identity, which warrants further exploration.

Finally, analysis in Figure 3 highlights substantial distributional differences between the MyGene2 and simulated datasets. When patients in the test set closely resemble training patients, prediction accuracy aligns across datasets. However, mismatches in patient phenotype distributions explain the performance gap observed between the datasets.

5 Conclusion

In this work, we proposed PhenoKG, a method that operates solely on patient phenotype data to produce a ranked list of potential causative genes, enabling the identification of novel or previously unobserved phenotype–gene associations

Table 2: Evaluation results using MRR and nDCG@K (in %) are reported across different model groups for the MyGene2 dataset. Higher values indicate better performance. The *Pretrained embeddings* group corresponds to training initialized with embeddings pretrained on the knowledge graph for a link prediction task. The *No embeddings* group refers to training from scratch. The *Only patient phenotypes* group includes models trained solely on original patient phenotype data. Rows within each group represent different training setups using various loss function combinations.

Model	MRR \uparrow	nDCG@1 \uparrow	nDCG@3 \uparrow	nDCG@5 \uparrow	nDCG@10 \uparrow	nDCG@25 \uparrow	nDCG@50	nDCG@75	nDCG@100
Competitive Method									
SHEPHERD	19.02 \pm 0.00	11.57 \pm 0.00	15.42 \pm 0.00	17.37 \pm 0.00	19.28 \pm 0.00	27.45 \pm 0.00	29.21 \pm 0.00	30.03 \pm 0.00	30.54 \pm 0.00
PhenoKG (Ours)									
$\mathcal{L}_{\text{gene}} \mathcal{L}_{\text{sim}}$									
<i>No Embeddings</i>									
✓ ✗	5.74 \pm 0.99	1.65 \pm 0.67	2.69 \pm 1.19	3.95 \pm 1.12	5.74 \pm 0.87	9.39 \pm 1.27	12.77 \pm 1.62	14.62 \pm 2.19	16.19 \pm 2.09
✗ ✓	7.27 \pm 2.47	2.75 \pm 0.78	5.15 \pm 2.40	6.28 \pm 3.25	7.87 \pm 3.89	10.36 \pm 3.56	12.53 \pm 2.75	14.47 \pm 2.18	15.54 \pm 2.31
✓ ✓	5.87 \pm 0.94	2.48 \pm 0.67	3.76 \pm 0.46	4.32 \pm 1.07	5.87 \pm 0.90	7.97 \pm 1.76	11.69 \pm 1.77	13.49 \pm 1.92	14.59 \pm 1.63
<i>Only Patient Phenotypes</i>									
✓ ✗	21.52 \pm 1.76	11.02 \pm 2.81	20.00 \pm 1.39	21.72 \pm 1.63	25.30 \pm 1.53	28.38 \pm 1.27	29.48 \pm 1.38	30.22 \pm 1.10	30.78 \pm 1.54
✗ ✓	19.19 \pm 0.88	7.16 \pm 0.39	16.55 \pm 0.96	20.60 \pm 0.87	25.07 \pm 1.78	27.13 \pm 0.59	28.81 \pm 0.64	29.73 \pm 0.81	30.28 \pm 0.79
✓ ✓	19.49 \pm 1.56	8.54 \pm 2.55	16.55 \pm 0.62	20.02 \pm 2.12	24.28 \pm 1.38	27.18 \pm 1.34	29.43 \pm 1.11	30.08 \pm 1.04	30.59 \pm 0.95
<i>Pretrained Embeddings</i>									
✓ ✗	23.40 \pm 1.43	13.22 \pm 1.17	21.71 \pm 0.72	25.02 \pm 1.85	27.10 \pm 3.05	29.68 \pm 2.49	30.86 \pm 1.81	31.55 \pm 1.52	32.41 \pm 1.67
✗ ✓	21.13 \pm 2.63	10.19 \pm 2.55	18.10 \pm 3.42	22.60 \pm 3.42	25.52 \pm 2.91	28.83 \pm 2.27	30.58 \pm 1.81	31.15 \pm 1.68	31.53 \pm 1.77
✓ ✓	24.64 \pm 4.57	15.15 \pm 3.33	22.74 \pm 5.28	25.33 \pm 5.40	28.17 \pm 4.73	30.86 \pm 4.40	32.30 \pm 4.42	33.04 \pm 4.32	33.64 \pm 4.64

not explicitly represented in the knowledge graph. The method does not rely on genetic data or predefined candidate lists and outperforms existing approaches across multiple gene prioritization metrics. It can be used as a pre-filter to narrow the search space before variant analysis and, following this pre-filtering, as a gene prioritization tool to rank the remaining candidate genes. However, while it exceeds recent state-of-the-art methods without candidate genes, its performance remains insufficient for standalone clinical application and is better suited as part of a multi-step filtering and prioritization pipeline.

References

- David R Adams, Clara DM van Karnebeek, Sergi Beltran Agullo, Víctor Faundes, Saumya Shekhar Jamuar, Sally Ann Lynch, Guillem Pintos-Morell, Ratna Dua Puri, Ruty Shai, Charles A Steward, et al. Addressing diagnostic gaps and priorities of the global rare diseases community: Recommendations from the irdirc diagnostics scientific committee. *European Journal of Medical Genetics*, page 104951, 2024.
- Bronwen L Aken, Sarah Ayling, Daniel Barrell, Laura Clarke, Valery Curwen, Susan Fairley, Julio Fernandez Banet, Konstantinos Billis, Carlos García Girón, Thibaut Hourlier, et al. The ensembl gene annotation system. *Database*, 2016:baw093, 2016.
- Emily Alsentzer, Michelle M Li, Shilpa N Kobren, Ayush Noori, Undiagnosed Diseases Network, Isaac S Kohane, and Marinka Zitnik. Few shot learning for phenotype-driven diagnosis of patients with rare genetic diseases. *medRxiv*, pages 2022–12, 2022.
- Emily Alsentzer, Samuel G Finlayson, Michelle M Li, Undiagnosed Diseases Network, Shilpa N Kobren, and Isaac S Kohane. Simulation of undiagnosed patients with novel genetic conditions. *Nature Communications*, 14(1):6403, 2023.
- Denise Anderson, Gareth Baynam, Jenefer M Blackwell, and Timo Lassmann. Personalised analytics for rare disease diagnostics. *Nature communications*, 10(1):5274, 2019.
- Jimmy Lei Ba, Jamie Ryan Kiros, and Geoffrey E Hinton. Layer normalization. *arXiv preprint arXiv:1607.06450*, 2016.
- Johannes Birgmeier, Maximilian Haeussler, Cole A Deisseroth, Ethan H Steinberg, Karthik A Jagadeesh, Alexander J Ratner, Harendra Guturu, Aaron M Wenger, Mark E Diekhans, Peter D Stenson, et al. Amelie speeds mendelian diagnosis by matching patient phenotype and genotype to primary literature. *Science Translational Medicine*, 12(544):eaau9113, 2020.

- Kym M Boycott, Megan R Vanstone, Dennis E Bulman, and Alex E MacKenzie. Rare-disease genetics in the era of next-generation sequencing: discovery to translation. *Nature Reviews Genetics*, 14(10):681–691, 2013.
- Shaked Brody, Uri Alon, and Eran Yahav. How attentive are graph attention networks? In *International Conference on Learning Representations*, 2022. URL <https://openreview.net/forum?id=F72ximsx7C1>.
- Payal Chandak, Kexin Huang, and Marinka Zitnik. Building a knowledge graph to enable precision medicine. *Scientific Data*, 10(1):67, 2023.
- Jessica X Chong, Kati J Buckingham, Shalini N Jhangiani, Corinne Boehm, Nara Sobreira, Joshua D Smith, Tanya M Harrell, Margaret J McMillin, Wojciech Wiszniewski, Tomasz Gambin, et al. The genetic basis of mendelian phenotypes: discoveries, challenges, and opportunities. *The American Journal of Human Genetics*, 97(2):199–215, 2015.
- Sergio Decherchi, Elena Pedrini, Marina Mordenti, Andrea Cavalli, and Luca Sangiorgi. Opportunities and challenges for machine learning in rare diseases. *Frontiers in medicine*, 8:747612, 2021.
- Dat Duong, Ping Hu, Cedrik Tekendo-Ngongang, Suzanna E Ledgister Hanchard, Simon Liu, Benjamin D Solomon, and Rebekah L Waikel. Neural networks for classification and image generation of aging in genetic syndromes. *Frontiers in genetics*, 13:864092, 2022.
- William A Gahl, Thomas C Markello, Camilo Toro, Karin Fuentes Fajardo, Murat Sincan, Fred Gill, Hannah Carlson-Donohoe, Andrea Gropman, Tyler Mark Pierson, Gretchen Golas, et al. The national institutes of health undiagnosed diseases program: insights into rare diseases. *Genetics in medicine*, 14(1):51–59, 2012.
- Yaron Gurovich, Yair Hanani, Omri Bar, Guy Nadav, Nicole Fleischer, Dekel Gelbman, Lina Basel-Salmon, Peter M Krawitz, Susanne B Kamphausen, Martin Zenker, et al. Identifying facial phenotypes of genetic disorders using deep learning. *Nature medicine*, 25(1):60–64, 2019.
- Dian Hong, Ying-Yi Zheng, Ying Xin, Ling Sun, Hang Yang, Min-Yin Lin, Cong Liu, Bo-Ning Li, Zhi-Wei Zhang, Jian Zhuang, et al. Genetic syndromes screening by facial recognition technology: Vgg-16 screening model construction and evaluation. *Orphanet Journal of Rare Diseases*, 16:1–8, 2021.
- Tzung-Chien Hsieh, Martin A Mensah, Jean T Pantel, Dione Aguilar, Omri Bar, Allan Bayat, Luis Becerra-Solano, Heidi B Bentzen, Saskia Biskup, Oleg Borisov, et al. Pedia: prioritization of exome data by image analysis. *Genetics in Medicine*, 21(12):2807–2814, 2019.
- Tzung-Chien Hsieh, Aviram Bar-Haim, Shahida Moosa, Nadja Ehmke, Karen W Gripp, Jean Tori Pantel, Magdalena Danyel, Martin Atta Mensah, Denise Horn, Stanislav Rosnev, et al. Gestaltmatcher facilitates rare disease matching using facial phenotype descriptors. *Nature genetics*, 54(3):349–357, 2022.
- Karthik A Jagadeesh, Aaron M Wenger, Mark J Berger, Harendra Guturu, Peter D Stenson, David N Cooper, Jonathan A Bernstein, and Gill Bejerano. M-cap eliminates a majority of variants of uncertain significance in clinical exomes at high sensitivity. *Nature genetics*, 48(12):1581–1586, 2016.
- Karthik A Jagadeesh, Johannes Birgmeier, Harendra Guturu, Cole A Deisseroth, Aaron M Wenger, Jonathan A Bernstein, and Gill Bejerano. Phrank measures phenotype sets similarity to greatly improve mendelian diagnostic disease prioritization. *Genetics in Medicine*, 21(2):464–470, 2019.
- Regis A James, Ian M Campbell, Edward S Chen, Philip M Boone, Mitchell A Rao, Matthew N Bainbridge, James R Lupski, Yaping Yang, Christine M Eng, Jennifer E Posey, et al. A visual and curatorial approach to clinical variant prioritization and disease gene discovery in genome-wide diagnostics. *Genome medicine*, 8:1–17, 2016.
- Kalervo Järvelin and Jaana Kekäläinen. Cumulated gain-based evaluation of ir techniques. *ACM Transactions on Information Systems (TOIS)*, 20(4):422–446, 2002.
- Asif Javed, Saloni Agrawal, and Pauline C Ng. Phen-gen: combining phenotype and genotype to analyze rare disorders. *Nature methods*, 11(9):935–937, 2014.
- Sebastian Köhler, Marcel H Schulz, Peter Krawitz, Sebastian Bauer, Sandra Dölken, Claus E Ott, Christine Mundlos, Denise Horn, Stefan Mundlos, and Peter N Robinson. Clinical diagnostics in human genetics with semantic similarity searches in ontologies. *The American Journal of Human Genetics*, 85(4):457–464, 2009.

- Sebastian Köhler, Leigh Carmody, Nicole Vasilevsky, Julius O B Jacobsen, Daniel Danis, Jean-Philippe Gouridine, Michael Gargano, Nomi L Harris, Nicolas Matentzoglou, Julie A McMurry, et al. Expansion of the human phenotype ontology (hpo) knowledge base and resources. *Nucleic acids research*, 47(D1):D1018–D1027, 2019.
- Alex Krizhevsky, Ilya Sutskever, and Geoffrey E Hinton. Imagenet classification with deep convolutional neural networks. *Advances in neural information processing systems*, 25, 2012.
- Qigang Li, Keyan Zhao, Carlos D Bustamante, Xin Ma, and Wing H Wong. Xrare: a machine learning method jointly modeling phenotypes and genetic evidence for rare disease diagnosis. *Genetics in Medicine*, 21(9):2126–2134, 2019.
- Ilya Loshchilov and Frank Hutter. Sgdr: Stochastic gradient descent with warm restarts. *arXiv preprint arXiv:1608.03983*, 2016.
- Ilya Loshchilov and Frank Hutter. Decoupled weight decay regularization. *arXiv preprint arXiv:1711.05101*, 2017.
- Andrew L Maas, Awni Y Hannun, Andrew Y Ng, et al. Rectifier nonlinearities improve neural network acoustic models. In *Proc. icml*, volume 30, page 3. Atlanta, GA, 2013.
- Dongxue Mao, Chaozhong Liu, Linhua Wang, Rami Al-Ouran, Cole Deisseroth, Sasidhar Pasupuleti, Seon Young Kim, Lucian Li, Jill A Rosenfeld, Linyan Meng, et al. Ai-marrvel—a knowledge-driven ai system for diagnosing mendelian disorders. *NEJM AI*, 1(5):A10a2300009, 2024.
- Stéphanie Nguengang Wakap, Deborah M Lambert, Annie Olry, Charlotte Rodwell, Charlotte Gueydan, Valérie Lanneau, Daniel Murphy, Yann Le Cam, and Ana Rath. Estimating cumulative point prevalence of rare diseases: analysis of the orphanet database. *European journal of human genetics*, 28(2):165–173, 2020.
- Chengyao Peng, Simon Dieck, Alexander Schmid, Ashar Ahmad, Alexej Knaus, Maren Wenzel, Laura Mehnert, Birgit Zirn, Tobias Haack, Stephan Ossowski, et al. Cada: phenotype-driven gene prioritization based on a case-enriched knowledge graph. *NAR Genomics and Bioinformatics*, 3(3):lqab078, 2021.
- Jennifer E Posey, Anne H O’Donnell-Luria, Jessica X Chong, Tamar Harel, Shalini N Jhangiani, Zeynep H Coban Akdemir, Steven Buyske, Davut Pehlivan, Claudia MB Carvalho, Samantha Baxter, et al. Insights into genetics, human biology and disease gleaned from family based genomic studies. *Genetics in Medicine*, 21(4):798–812, 2019.
- PKS Prakash, Srinivas Chilukuri, Nikhil Ranade, and Shankar Viswanathan. Rarebert: transformer architecture for rare disease patient identification using administrative claims. In *Proceedings of the AAAI conference on artificial intelligence*, volume 35, pages 453–460, 2021.
- Rachel B Ramoni, John J Mulvihill, David R Adams, Patrick Allard, Euan A Ashley, Jonathan A Bernstein, William A Gahl, Rizwan Hamid, Joseph Loscalzo, Alexa T McCray, et al. The undiagnosed diseases network: accelerating discovery about health and disease. *The American Journal of Human Genetics*, 100(2):185–192, 2017.
- Aditya Rao, Saipradeep Vg, Thomas Joseph, Sujatha Kotte, Naveen Sivadasan, and Rajgopal Srinivasan. Phenotype-driven gene prioritization for rare diseases using graph convolution on heterogeneous networks. *BMC medical genomics*, 11:1–12, 2018.
- Philipp Rentzsch, Daniela Witten, Gregory M Cooper, Jay Shendure, and Martin Kircher. Cadd: predicting the deleteriousness of variants throughout the human genome. *Nucleic acids research*, 47(D1):D886–D894, 2019.
- Sue Richards, Nazneen Aziz, Sherri Bale, David Bick, Soma Das, Julie Gastier-Foster, Wayne W Grody, Madhuri Hegde, Elaine Lyon, Elaine Spector, et al. Standards and guidelines for the interpretation of sequence variants: a joint consensus recommendation of the american college of medical genetics and genomics and the association for molecular pathology. *Genetics in medicine*, 17(5):405–423, 2015.
- Peter N Robinson, Vida Ravanmehr, Julius OB Jacobsen, Daniel Danis, Xingmin Aaron Zhang, Leigh C Carmody, Michael A Gargano, Courtney L Thaxton, Guy Karlebach, Justin Reese, et al. Interpretable clinical genomics with a likelihood ratio paradigm. *The American Journal of Human Genetics*, 107(3):403–417, 2020.
- Pushkar Shukla, Tanu Gupta, Aradhya Saini, Priyanka Singh, and Raman Balasubramanian. A deep learning frame-work for recognizing developmental disorders. In *2017 IEEE Winter Conference on Applications of Computer Vision (WACV)*, pages 705–714. IEEE, 2017.

- Damian Smedley, Julius OB Jacobsen, Marten Jäger, Sebastian Köhler, Manuel Holtgrewe, Max Schubach, Enrico Siragusa, Tomasz Zemojtel, Orion J Buske, Nicole L Washington, et al. Next-generation diagnostics and disease-gene discovery with the exomiser. *Nature protocols*, 10(12):2004–2015, 2015.
- Robin Steinhaus, Sebastian Proft, Markus Schuelke, David N Cooper, Jana Marie Schwarz, and Dominik Seelow. Mutationtaster2021. *Nucleic Acids Research*, 49(W1):W446–W451, 2021.
- Natasha T Strande, Erin Rooney Riggs, Adam H Buchanan, Ozge Ceyhan-Birsoy, Marina DiStefano, Selina S Dwight, Jenny Goldstein, Rajarshi Ghosh, Bryce A Seifert, Tam P Sneddon, et al. Evaluating the clinical validity of gene-disease associations: an evidence-based framework developed by the clinical genome resource. *The American Journal of Human Genetics*, 100(6):895–906, 2017.
- Will E Thompson, David M Vidmar, Jessica K De Freitas, John M Pfeifer, Brandon K Fornwalt, Ruijun Chen, Gabriel Altay, Kabir Manghnani, Andrew C Nelsen, Kellie Morland, et al. Large language models with retrieval-augmented generation for zero-shot disease phenotyping. *arXiv preprint arXiv:2312.06457*, 2023.
- University of Washington, Center for Mendelian Genomics. Mygene2. <https://www.mygene2.org/MyGene2/>. Accessed: 2025-05-12.
- Ashish Vaswani, Noam Shazeer, Niki Parmar, Jakob Uszkoreit, Llion Jones, Aidan N Gomez, Łukasz Kaiser, and Illia Polosukhin. Attention is all you need. *Advances in neural information processing systems*, 30, 2017.
- Hui Yang, Peter N Robinson, and Kai Wang. Phenolyzer: phenotype-based prioritization of candidate genes for human diseases. *Nature methods*, 12(9):841–843, 2015.
- Boyoung Yoo, Johannes Birgmeier, Jonathan A Bernstein, and Gill Bejerano. Inphernet accelerates monogenic disease diagnosis using patients’ candidate genes’ neighbors. *Genetics in Medicine*, 23(10):1984–1992, 2021.